



Solar and volcanic forcing of North Atlantic climate inferred from a process-based reconstruction

Jesper Sjolte¹, Christophe Sturm², Florian Adolphi^{1,3}, Bo M. Vinther⁴, Martin Werner⁵, Gerrit Lohmann⁵, and Raimund Muscheler¹

¹Department of Geology – Quaternary Science, Lund University, Sölvegatan 12, 223 62, Lund, Sweden.

²Department of Geological Sciences, Stockholm University, SE-106 91 Stockholm, Sweden.

³Climate and Environmental Physics & Oeschger Centre for Climate Change Research, Physics Institute, University of Bern, Sidlerstrasse 5, CH-3012 Bern, Switzerland

⁴Centre for Ice and Climate, Niels Bohr Institute, University of Copenhagen, Juliane Maries Vej 30, DK-2100 Copenhagen Oe, Denmark.

⁵Alfred Wegener Institute, Helmholtz Centre for Polar and Marine Sciences, Postfach 12 01 61, 27515 Bremerhaven, Germany.

Correspondence: Jesper Sjolte (jesper.sjolte@geol.lu.se)

Abstract. External forcings are known to impact atmospheric circulation. However, the analysis of the role of external forcings based on observational data is hampered due to the short observational period, and the sensitivity of atmospheric circulation to external forcings as well as persistence the effects are debated. A positive phase of the North Atlantic Oscillation (NAO) has been observed the following winter after tropical volcanic eruptions. However, past major tropical eruptions exceeding the magnitude of eruptions during the instrumental era could have more lasting effects. Decadal NAO variability has been suggested to follow the 11-year solar cycle, and linkages has been made between grand solar minima and negative NAO. However, the solar link to NAO found by modeling studies is not unequivocally supported by reconstructions, and is not consistently present in observations for the 20th century. Here we present a reconstruction of atmospheric winter circulation for the North Atlantic region covering the period 1241-1970 CE. Based on seasonally resolved Greenland ice core records and a 1200-year long simulation with an isotope enabled climate model, we reconstruct sea level pressure and temperature by matching the spatio-temporal variability of the modeled isotopic composition to that of the ice cores. This method allows us to capture the primary and secondary modes of atmospheric circulation in the North Atlantic region, while, contrary to previous reconstructions, preserving the amplitude of observed year-to-year atmospheric variability. Our results show 5 winters of positive NAO on average following major tropical volcanic eruptions, which is more persistent than previously suggested. In response to decadal minima of solar activity we find a high-pressure anomaly over Northern Europe, while a reinforced opposite response in pressure emerges with a 5-year time lag. On longer time scales we observe a similar response in circulation as for the 5-year time-lagged response. This is likely due to an increase in blocking frequency and an associated weakening of the subpolar gyre. The long-term response of temperature to solar minima shows cooling across Greenland, Iceland and Western Europe, resembling the cooling pattern during the Little Ice Age. While our results show a clear link between solar forcing and the secondary circulation patterns, we find no consistent relationship between solar forcing and NAO.



1 Introduction

Climate variability in the North Atlantic region can, to a large extent, be explained by different modes of atmospheric circulation. The dominant mode is the NAO, which is a measure of the strength and position of the westerly winds across the North Atlantic. Secondary modes of circulation include Atlantic Ridge and Trough -types of variability, characterized by mid-Atlantic and Scandinavian blockings, respectively (Hurrell et al., 2013). These different modes for example determine the severity of European winters (Hurrell et al., 2013). Past changes in climate and atmospheric circulation are often attributed to external forcing related to solar variability or volcanic eruptions. Using reanalysis of weather observations (1871-2008) it has been shown that a positive phase of the NAO occurs in the winters following major tropical volcanic eruptions, while climate models generally fail to reproduce this dynamical response to the forcing (Driscoll et al., 2012; Zambri and Robock, 2016; Swingedouw et al., 2017). For the past millennium Ortega et al. (2015) found a positive NAO response in the second winter following the 11 largest tropical eruptions in their reconstructed NAO. However, more persistent climate effects of volcanic eruptions were found by Sigl et al. (2015) who inferred cooler European summer temperatures lasting up to 10 years following major tropical eruptions during the past 2,500 years, raising the question if a more persistent impact on winter circulation also can be expected. The NAO has also been suggested to be influenced by solar forcing as anomalies in sea level pressure during 1950-2010 exhibit a NAO-like pattern correlated to the 11-year solar cycle (Ineson et al., 2011; Adolphi et al., 2014). It has been hypothesized that solar-induced anomalies in the stratosphere can propagate to the troposphere (Haigh and Blackburn, 2006; Kodera and Kuroda, 2005) possibly synchronizing NAO variability to the 11-year solar cycle (Thieblemont et al., 2015) with a maximum response lagging 2-4 years due to ocean memory effects (Scaife et al., 2013; Gray et al., 2013). Several paleoclimate studies have indicated solar influences on climate in the North Atlantic region on centennial time-scales (Bond et al., 2001; Sejrup et al., 2010; Moffa-Sanchez et al., 2014; Adolphi et al., 2014; Jiang et al., 2015), and it has been suggested that the climate conditions during the Little Ice Age was linked to negative NAO forced by low solar activity (Shindell et al., 2001; Swingedouw et al., 2011). However the nature of the solar influence in terms of mechanisms and dynamical response is debated.

Our understanding of past climate dynamics and the impact of external forcings relies heavily on analysis of past changes. Gridded data sets of climate variables based on meteorological observations have been developed for these purposes (Compo et al., 2011). Such reanalysis data sets are constrained in quality and coverage back in time due to sparse instrumental data, and we rely on climate reconstructions based on proxy data to go beyond the instrumental era. Previously, reconstructions of climate indices (such as e.g. the NAO) have been site-based, with the reconstruction essentially done by extrapolating observed empirical relationships back in time. This approach results in a wide spread of reconstructions of past atmospheric circulation modes (Pinto and Raible, 2012). Recently, efforts have been done to develop reanalysis-type climate reconstructions based on climate proxy data. However, those reconstructions are focused on annual mean data, not taking into account the migration of circulation patterns from summer to winter (Hurrell et al., 2013), and have low skill for atmospheric circulation over the North Atlantic (Hakim et al., 2016; Steiger et al., 2017).

Stable water isotope ratios in ice cores carry quantitative information about past climate (Johnsen and Vinther, 2007). For



Greenland ice cores seasonal isotope variability is attainable. In particular, the winter isotope signal has been shown to be highly correlated to atmospheric circulation and temperature (Vinther et al., 2003, 2010). However, the strength of the relation between the main patterns of variability of the ice core isotope signal and the NAO has been suggested to vary in strength (Vinther et al., 2003), indicating that a simple (regression based) relation between the ice core records and NAO bears large 5 uncertainties for reconstruction purposes.

Here we present a climate reconstruction for the North Atlantic region for winter covering 1241-1970 CE, and analyze the impact of solar and volcanic forcing. For our reconstruction we combine a simulation using a coupled atmosphere-ocean model with stable isotope diagnostics embedded in the hydrological cycle with eight seasonally resolved isotope records from Greenland ice cores. We do not calibrate the reconstructed meteorological variables to observations, as we solely rely on matching 10 the modeled isotopic composition to the ice core data. Testing the reconstruction against reanalysis data and observations, the reconstruction has good skill not only for the NAO, but also for secondary circulation modes. We find the average response to major tropical volcanic eruptions to be a positive NAO for the five consecutive winters after eruptions, which is more persistent than previous studies have shown. However, we find no persistent relationship between solar forcing and the NAO. On the other hand, we find a strong impact of solar forcing on the secondary modes of circulation represented by the second principal 15 component (PC2) of reconstructed sea level pressure (SLP). We achieve the strongest correspondence between the solar forcing and atmospheric circulation with time lag of 4-6 years, indicating that an ocean-atmosphere feedback is in play. Taking this time lag into account we find a consistent relationship between PC2 of reconstructed SLP and solar forcing on decadal to centennial time scales.

2 Data and Methods

20 2.1 Model simulation

We use the isotope enabled version of the atmosphere-ocean model ECHAM5/MPIOM (Werner et al., 2016) to simulate the period 800-2000 CE forced by greenhouse gases, volcanic aerosols, total solar irradiance, land-use and orbital forcing (see Table S1). Except for an updated solar forcing (see section below) and fully prescribed CO₂ the forcings are the same as for the E1 COSMOS ensemble by Jungclaus et al. (2010), generally yielding a very similar climate due to the identical physical 25 GCM models (ECHAM5/MPIOM) applied.

2.2 Solar forcing

The solar forcing record employed in this study is based on the solar modulation record inferred from the combined neutron monitor and tree-ring ¹⁴C data (Muscheler et al., 2016, 2007). In contrast to Schmidt et al. (2011, 2012) it covers the last 2000 years and consistently uses the solar modulation record for the complete period, while in Schmidt et al. (2011, 2012) the ¹⁴C- 30 based record is combined with sunspot-based data for the period after 1850 CE. Therefore, our approach employs an internally self-consistent forcing record for the last 2000 years, and agrees well with the latest recommended solar forcing reconstruction



for the past millennium (Jungclauss et al., 2017). The 11-year solar cycle is based on the neutron monitor and ^{14}C data for the last 500 years where the underlying data has a sufficiently high temporal resolution. For the period before 1500 CE an artificial 10.5-year cycle was added and the phasing was adjusted to allow for a smooth connection to the subsequent start of the data-based solar cycle. The amplitude of the solar cycle modulation was inferred from the data-based part of the record, i.e. by
5 employing the relationship between the solar cycle amplitude and the longer-term solar modulation levels (11-year averages) during last 500 years. This solar modulation record was scaled to the total solar irradiance (TSI) record by Schmidt et al. (2011, 2012) including longer-term trends in TSI (see “MEA (back)”, Figure 8 in Schmidt et al. (2011)). This was done by linearly transforming the solar modulation to a TSI record in order to reproduce the long-term changes (11-year average) in TSI from the Maunder minimum to the most recent 50 years i.e. leading to a similar range of long-term TSI changes as suggested by
10 Schmidt et al. (2011).

2.3 Climate reconstruction

We use winter seasonal means (Nov-Apr) for 8 Greenland ice cores (Vinther et al., 2010) for the period 1241-1970 CE (Table S2). All ice cores are synchronized via volcanic reference horizons, and the dating uncertainty is estimated to one year for the oldest parts of the records used here (Vinther et al., 2006). Under the assumption that $\delta^{18}\text{O}$ in precipitation is a result of a
15 number of processes mainly determined by atmospheric variability, we treat each year of the model run (see above) as a sample in a sampling space relating $\delta^{18}\text{O}$ in precipitation with circulation, temperature, etc. By extracting precipitation weighted winter seasonal means (Nov-Apr) of $\delta^{18}\text{O}$ from the model at the 8 ice cores sites we can find the model years best matching the isotope pattern of each winter in the ice core data. In order not to over-fit noise in the ice core data (post depositional processes etc. (White et al., 1997)) we first perform a principal component analysis of the ice core $\delta^{18}\text{O}$ and the model $\delta^{18}\text{O}$
20 from grid cells covering the investigated ice core sites. We retain the first three principal components (PCs) explaining a total of 60% and 97% of variability in the ice core and model $\delta^{18}\text{O}$, respectively. The loadings of the 3 PCs for the model data match the loading of the ice core data well (Figure S1). Notice that this step is done without performing any selection of the model data, meaning that the modeled spatio-temporal variability of the $\delta^{18}\text{O}$ in precipitation corresponds well to that of the ice core data. As we only explain part of the variability of the $\delta^{18}\text{O}$ data using the first 3 PCs, we use an ensemble approach to take into
25 account that the matching of a given ice core $\delta^{18}\text{O}$ pattern will result in a suite of well-matching model years. To match each year in the ice core data, the model data is evaluated using a χ^2 -measure between the 3 PCs of Greenland ice core $\delta^{18}\text{O}$ and the 3 PCs of the modeled $\delta^{18}\text{O}$:

$$\chi_{Match}^2 = \frac{1}{3} \sum_{k=1}^3 (PC(k)_{model} - PC(k)_{icecore})^2 \quad (1)$$

, where $PC(k)_{model}$ and $PC(k)_{icecore}$ are the values from a given year of the normalized time series of model and ice core
30 $\delta^{18}\text{O}$ PCs, respectively. Each model year is evaluated against each ice core year and then sorted in ascending order of the quality of the fit. This creates 1201 (number of model years, see above) fits of model data for each ice core year, and in turn 1201 resampled (with replacement) model fits for the entire length of the ice core data (1241-1970 CE). We view each of the fits along the length of the ice core data as ensemble members. Using a Chi-square goodness-of-fit test we evaluate the ensemble



members against the ice core data and reject model fits with likelihood $p > 0.01$ of not fitting the PCs of Greenland $\delta^{18}\text{O}$. This leaves us with 39 time series of model fits. The temporal succession of the reshuffled model fits do not resemble the order of the years in the original model, and there are no systematic preferences of the method to pick certain time periods of the model run to match certain time periods of the reconstruction. For example if we exclude the years 1851-2000 from the model run and perform the reconstruction using the remaining years, the reconstruction is almost identical to the reconstruction using all model years. This also means that the timing of the forcing used for the model run has no relation to the timing or impact of specific forcings in the reconstruction, i.e., the forcings of the model run effectively serve to produce enough range in order to match the simulation to the isotope variability of the ice cores. We treat the 39 model fits as an ensemble solution fitting the model output to the ice cores $\delta^{18}\text{O}$, and we calculate the ensemble mean reconstructed $\delta^{18}\text{O}$ and the standard deviation showing the ensemble spread. For the target climate variables (SLP, T2m) we extract the DJF ensemble mean corresponding to the reconstructed $\delta^{18}\text{O}$ constituting the reconstruction of these variables. Note that using this approach the method is optimized to fit modeled $\delta^{18}\text{O}$ to ice core $\delta^{18}\text{O}$ records and, in contrast to presently existing reconstructions, it is not calibrated to match observations of any of the target variables of the reconstruction (i.e. SLP or T2m).

As a first test we correlate the reconstructed $\delta^{18}\text{O}$ to winter means of ice core data from 20 cores covering the last 200 years of the reconstruction, i.e. including ice core data not part of the reconstruction. The correlation shows a spread between 0.4 and 0.9 with the highest correlations found for the high accumulation sites, supporting the idea that the skill of the model fit to the seasonal ice core data is largely limited by the signal-to-noise ratio of the ice core data (Figure S2). High accumulation sites are generally less sensitive to wind scouring and post depositional diffusion. Furthermore we test the fit of the reshuffled model $\delta^{18}\text{O}$ to the ice core data of the 8 sites to investigate if any time periods stand out, as well as the mean fit of the method across the whole period of the reconstruction. We find no trends in the performance in terms of fitting the modeled PCs to the ice core data PCs. As the method performs equally well during any period as during the instrumental period (post 1850) in terms of matching the ice core isotope variability, it is likely that our reconstruction of SLP and T2m is equally valid for any period as it is for the instrumental period. This conclusion can be drawn as the reconstruction is not calibrated to either SLP or T2m, and is only constrained by the ice core isotope variability.

25 3 Results

3.1 Evaluation of climate reconstruction

Comparing to the 20th Century Reanalysis (Compo et al., 2011) (20CR) our reconstruction shows skill for SLP and T2m in the North Atlantic region (Figure 1 a, b), the main mode of atmospheric circulation (NAO) as well as secondary circulation modes (Figure 1 c, d and Table 1). Note that our reconstruction is completely independent of the reanalysis data set. For T2m the pattern of significant correlations with the 20CR data is associated with the main circulation modes (Figure S3 and S4), albeit with decreasing skill with the distance to the ice cores. We interpret the high skill near Greenland as being due to the direct physical connection between the local temperature in Greenland and the temperature along the path of the vapor, and the isotopic signal in Greenland ice cores. Contrary to previous millennial scale reconstructions our reconstructed NAO shows similar strength of



year-to-year variability as the observed NAO indicating that the reconstruction preserves the known characteristic variability of the NAO (Figure 1 d, e, Figure 2 a). In addition to capturing the NAO, our reconstruction has skill in representing Atlantic ridge/trough-type variability as projected on PC2 of SLP over the North Atlantic. The correlation of the reconstructed SLP PC2 and PC2 of the 20CR SLP is 0.24 ($p < 0.01$) and increases to 0.53 ($p < 0.01$) on decadal time scales (Table 1). However, comparing the SLP patterns of PC2 in our reconstruction and reanalysis (Figure S3) implies that the variability captured by in PC2 of the reconstruction is likely split between PC2 and PC3 in the reanalysis. Indeed, the reconstructed PC2 of SLP is also correlated to PC3 of the reanalysis SLP (corr. = 0.19, $p < 0.01$, Table 1). Correlating the reconstructed PC2 of SLP against the sum of the reanalysis PC2 and PC3 shows increased correlations between the reconstruction and reanalysis, in particularly on decadal and bi-decadal time scales (Table 1). The difference in distribution of the variability on the PCs in the reconstruction and reanalysis is likely due to i) the intrinsic variability of the model use for the reconstruction and ii) the reconstruction only captures the North Atlantic variability as recorded in the isotopic composition of the Greenland ice core data.

The reconstructed NAO shows strong multi-decadal variability, while no major trends are found on centennial time scales, as opposed to the reconstruction by Trouet et al. (2009), and in agreement with the NAO reconstructions by Ortega et al. (2015) (Figure 2). The NAO reconstructions by Ortega et al. (2015) consists two multi-proxy NAO reconstructions. Of these reconstructions one is calibration-constrained (NAOcc) and the other model-constrained (NAOmc) (Figure 2 b), where NAOmc only uses proxies from sites that were estimated from model simulations to have a stable relation to the NAO. It should be noted that both the reconstruction by Ortega et al. (2015) and this study use some of the same Greenland ice core data (Crete, DYE-3, GRIP), which obviously could lead to a correspondence in variability. We find the NAO in our SLP reconstruction has best correspondence with NAOmc for interannual variability, while for multi-decadal time scales prior to the instrumental period, there is little coherency between our reconstruction and both NAOmc and NAOcc (Table 1). This lack of coherence of multidecadal variability is similar to the aforementioned divergence between previous NAO reconstructions. For an independent comparison we used gridded reconstructions of SLP (Luterbacher et al., 2001) and temperature (Luterbacher et al., 2004) over Europe. However, we restricted the comparison to 1659-1970 due to the methodological differences in the reconstructions for Europe prior and post 1659, and the use of Greenland ice core data for the European temperature reconstruction covering 1500-1658. The comparison between our reconstruction and these reconstructions for Europe shows similar pattern and correlation levels for SLP as with the 20CR data, and moderate, but significant, correlations for temperature (Figure S5).

Our reconstructed NAO shows higher correlation (corr. = 0.52, $p < 0.01$) to the observed NAO (Jones et al., 1997) (DJF, 1824-1970) than NAOmc and NAOcc, which have correlations to the observed NAO of 0.46 and 0.47, respectively. Even more important, the skill of our reconstructed NAO is achieved without calibrating to the observed NAO. In summary, we think that our reconstruction is the most suitable for analyzing the influence of volcanic eruptions and solar activity on circulation, because i) our reconstruction not only has good skill for the NAO, but also for the secondary modes of circulation, which, as we will show later, is crucial for investigating the impact of solar forcing ii) high frequency variability is preserved, making it possible better to detect rapid shifts in circulation after volcanic eruptions, and finally iii) our reconstruction is not calibrated to observed SLP or T2m, making it free of biases that could arise from tuning a reconstruction to observations during the instrumental era.



3.2 Response of atmospheric circulation to external forcing

In this section we investigate the reconstructed response in SLP and temperature to major tropical volcanic eruptions and solar variability. The mean post eruption SLP and T2m anomalies in response to 12 major tropical eruptions show the characteristics of a positive NAO (Figure 3 a, b). On average, we find a significant positive NAO response during the five consecutive winters following the eruptions (Figure 3 c). Performing the same analysis on NAOmc yields a similar response, while not reaching as high significance levels and persistence as our reconstruction, likely due to the attenuated year-to-year variability of NAOmc (Figure 1 c & 3 c, Figure S6). Due to the short time span between some of the volcanic eruptions it is not possible to consistently analyze any longer term response than five years, since it would limit the number of eruptions and, hence, the robustness of the statistical analysis. However, together with the suggested 5-10 years of post eruption summer cooling in Europe (Sigl et al., 2015), our result points to a persistence in the response to major tropical volcanic eruptions we have yet to observe in the instrumental record.

For the analysis of solar influences on circulation we analyzed the average response to the 11-year solar cycle and the multi-decadal to centennial solar variability. We calculated the difference between reconstructed SLP and T2m for years of low and high solar activity using the annual sunspot number (Clette and Lefèvre, 2016) (1700-1970) and a ^{14}C -based solar reconstruction (1241-1970) (see Sect. 2.2) for the short term and long term cycles, respectively. The response to the 11-year solar cycle (solar low minus high) is a Scandinavian blocking-type pattern corresponding well to the pattern found for reanalysis data (Figure 4 a, d and Figure 5 a, c). Investigating the time lagged response to the 11-year solar cycle we find the strongest response in reconstructed SLP and T2m when lagging the solar forcing with 5 years, which also matches the time lagged pattern found in reanalysis data (Figure 4 b, e and Figure 5 b, d). This pattern projects on PC2 of the reconstructed SLP, also with the strongest correlation between forcing and response when lagging the sunspot data with 5 years. Taking this time lag into account yields a consistent relationship between solar forcing and PC2 of reconstructed SLP on decadal to multi-decadal time scales (Figure 6, Table 2). It should be noted that the 5-year lagged response in circulation is not simply due to the response to the solar maximum approximately half a cycle later in the 11-year solar cycle, but a reinforced response. This is most clearly seen in the stronger correlations for the time lagged response, both for the original data and the filtered data (Table 2). The relation between PC2 of reconstructed SLP and solar forcing persists also for centennial variability, which is seen by comparing the circulation response to the ^{14}C -based solar reconstruction (Table 2, Figure S7). The pattern of the response in SLP to the long-term solar minima is an Atlantic ridge-type pattern (anomalous high south of Greenland), which also projects on PC2 of SLP, with an associated cooling pattern for the western North Atlantic (Figure 4 c, f). Compared to the 5-year lagged response to the 11-year cycle this pattern has the strongest response in SLP south of Greenland, with a similar, but more widespread cooling in the eastern North Atlantic. Even though the SLP response looks slightly different for short and long-term solar forcing variations, the main feature: a wave structure over the North Atlantic and Scandinavia, is consistent. The temperature response to the long-term solar minima is a cooling across Greenland, Iceland and western Europe during solar minima (Figure 4 f). This cooling pattern corresponds well to the suggested cooling during the Little Ice Age in proxy records from Greenland (Stuiver et al., 1997), Iceland (Moffa-Sanchez et al., 2014) and Europe (Luterbacher et al., 2004). A NAO-type response to



long-term solar forcing would give opposing temperature responses in Greenland and Europe, which is not the case. We find no consistent relation between our reconstructed NAO and solar forcing. Instead we would like to stress the importance of the connection between solar activity and the secondary circulation patterns, which likely captures the main response to solar forcing on decadal to centennial time scales.

5 4 Discussion

Model studies of the volcanic response to major tropical eruptions during the past millennium show a large spread in the modeled NAO/AO response, with either no consistent response or 1-2 years of significant response (Swingedouw et al., 2017; Zambri et al., 2017). In contrast to this we find a clear tendency for positive NAO for the five consecutive winters following the year of eruption as an average response to the 12 largest tropical eruptions during 1241-1970 CE. An immediate strengthening of the polar vortex following eruptions is in agreement with the observed response of atmospheric circulation (Driscoll et al., 2012), which then translates to a positive NAO as the stratospheric anomaly propagates to the troposphere. The presence of volcanic aerosols gradually tails off of during the first 2-3 years (Crowley and Unterman, 2013) and a more sustained positive NAO for up to five years can best be explained via a positive ocean feedback through a tri-pole SST response to the strongly anomalous positive NAO (Cayan, 1992). Ongoing efforts to improve the simulation of volcanic forcing and response could help close the gap between models and observations as well as reconstructions (Zanchettin et al., 2016).

It has been suggested that the observed increase in blocking frequency over the North Atlantic in response to solar minima (Woollings et al., 2010) is coupled to a weakening of the polar night jet in response to a weaker stratospheric equator-pole temperature gradient. This mechanism could be in play on both decadal and centennial time scales. A recent study investigated the response in circulation to solar activity using a regression-based analysis between sunspot data and gridded observed SLP and SST data (Gray et al., 2016). The authors analyzed the time lagged response to solar forcing, and found that the solar response could be explained via two mechanisms (Gray et al., 2016). One involving the aforementioned stratosphere-troposphere coupling acting on time lags of 0-2 years, and one for time lags of 3-4 years involving ocean temperature anomalies being stored beneath the mixed layer and reinforced from the previous winter (Gray et al., 2016). The reinforcement of SST anomalies from year-to-year has also been shown in a simulation of the response to the solar 11-year cycle (Andrews et al., 2015). Such a mechanism could be the cause of the time lag we see in the reconstructed response to solar forcing, although we get the maximum response at 5-year time lag, compared to the 3-4 year time lag found in observations (Gray et al., 2016). However, this difference could be due to differences in the methodologies of the analysis of the response to solar forcing, and that the aforementioned study (Gray et al., 2016) is focusing on the NAO-like response seen in their analysis. A likely mechanism based on our findings is as follows. An initial increase in atmospheric blockings weakens the subpolar gyre (Moffa-Sanchez et al., 2014) (SPG), thereby decreasing the heat transport to the north-western North Atlantic giving favorable conditions for mid-Atlantic blocking. This pattern is reinforced year-by-year and the main atmospheric response shifts to the node of PC2 of SLP south of Greenland under sustained forcing conditions on longer time scales (Figure 4 c). A recent model study (Moreno-Chamarro et al., 2017) suggested that the cooling during the Little Ice Age was connected to a weakening in the SPG, sustained by way of atmosphere-



- ocean feedbacks. Although the authors do not related this to solar forcing, but with preconditioned initial model variability, the anomalies in SLP and temperature associated with the weakening of the SPG are very similar to the reconstructed pattern of the response to long-term solar forcing. Our study of the reconstructed North Atlantic winter circulation shows a complex response to solar forcing which is, in contrast to a prevalent hypothesis, not directly linked to the NAO. In our study we do not
- 5 exclude that there could be an influence of the solar 11-year cycle on NAO. However, unlike for PC2 of reconstructed SLP, we find no consistent relationship between reconstructed NAO and solar forcing across multiple time scales. Furthermore, the results suggest that sustained longer-term solar forcing leads to a shift in the atmospheric circulation response compared to the response to the short-term forcing, likely due to feedback processes involving the ocean integrating the long term effects of anomalous atmospheric circulation.
- 10 *Author contributions.* J.S. developed the method, performed the analysis, conducted the model simulation and wrote the first version of the manuscript. C.S. initiated the study and contributed to setting up the model simulation. F.A. contributed to the method development and analysis. B.V. provided seasonal ice core data. M.W. provided technical support for model simulation and access to climate model. G.L. provided insights on model setup. R.M. contributed with solar activity reconstruction and provided insight on solar forcing of climate. All authors discussed and edited the manuscript.
- 15 *Competing interests.* The authors declare no competing interests.

Acknowledgements. This work was supported by the Swedish Research Council (grant DNR2011-5418 & DNR2013-8421 to RM), the Crafoord foundation and the strategic research program of ModEling the Regional and Global Earth system (MERGE) hosted by the Faculty of Science at Lund University. The model simulation was carried out at the AWI Computer and Data Center, Bremerhaven.



References

- Adolphi, F., Muscheler, R., Svensson, A., Aldahan, A., Possnert, G., Beer, J., Sjolte, J., Bjorck, S., Matthes, K., and Thieblemont, R.: Persistent link between solar activity and Greenland climate during the Last Glacial Maximum, *NATURE GEOSCIENCE*, 7, 662–666, <https://doi.org/10.1038/NGEO2225>, 2014.
- 5 Andrews, M. B., Knight, J. R., and Gray, L. J.: A simulated lagged response of the North Atlantic Oscillation to the solar cycle over the period 1960–2009, *Environmental Research Letters*, 10, 054 022, <http://stacks.iop.org/1748-9326/10/i=5/a=054022>, 2015.
- Bond, G., Kromer, B., Beer, J., Muscheler, R., Evans, M., Showers, W., Hoffmann, S., Lotti-Bond, R., Hajdas, I., and Bonani, G.: Persistent solar influence on north Atlantic climate during the Holocene, *SCIENCE*, 294, 2130–2136, <https://doi.org/10.1126/science.1065680>, 2001.
- Cayan, D. R.: LATENT AND SENSIBLE HEAT-FLUX ANOMALIES OVER THE NORTHERN OCEANS - DRIVING THE SEA-SURFACE TEMPERATURE, *JOURNAL OF PHYSICAL OCEANOGRAPHY*, 22, 859–881, [https://doi.org/10.1175/1520-0485\(1992\)022<0859:LASHFA>2.0.CO;2](https://doi.org/10.1175/1520-0485(1992)022<0859:LASHFA>2.0.CO;2), 1992.
- 10 Clette, F. and Lefèvre, L.: The New Sunspot Number: Assembling All Corrections, *Solar Physics*, 291, 2629–2651, <https://doi.org/10.1007/s11207-016-1014-y>, <https://doi.org/10.1007/s11207-016-1014-y>, 2016.
- Compo, G. P., Whitaker, J. S., Sardeshmukh, P. D., Matsui, N., Allan, R. J., Yin, X., Gleason, Jr., B. E., Vose, R. S., Rutledge, G., Bessemoulin, P., Broennimann, S., Brunet, M., Crouthamel, R. I., Grant, A. N., Groisman, P. Y., Jones, P. D., Kruk, M. C., Kruger, A. C., Marshall, G. J., Maugeri, M., Mok, H. Y., Nordli, O., Ross, T. F., Trigo, R. M., Wang, X. L., Woodruff, S. D., and Worley, S. J.: The Twentieth Century Reanalysis Project, *QUARTERLY JOURNAL OF THE ROYAL METEOROLOGICAL SOCIETY*, 137, 1–28, <https://doi.org/10.1002/qj.776>, 2011.
- 15 Crowley, T. J. and Unterman, M. B.: Technical details concerning development of a 1200 yr proxy index for global volcanism, *EARTH SYSTEM SCIENCE DATA*, 5, 187–197, <https://doi.org/10.5194/essd-5-187-2013>, 2013.
- 20 Driscoll, S., Bozzo, A., Gray, L. J., Robock, A., and Stenchikov, G.: Coupled Model Intercomparison Project 5 (CMIP5) simulations of climate following volcanic eruptions, *JOURNAL OF GEOPHYSICAL RESEARCH-ATMOSPHERES*, 117, <https://doi.org/10.1029/2012JD017607>, 2012.
- Ebisuzaki, W.: A method to estimate the statistical significance of a correlation when the data are serially correlated, *JOURNAL OF CLIMATE*, 10, 2147–2153, [https://doi.org/10.1175/1520-0442\(1997\)010<2147:AMTETS>2.0.CO;2](https://doi.org/10.1175/1520-0442(1997)010<2147:AMTETS>2.0.CO;2), 1997.
- 25 Gray, L. J., Woollings, T. J., Andrews, M., and Knight, J.: Eleven-year solar cycle signal in the NAO and Atlantic/European blocking, *Quarterly Journal of the Royal Meteorological Society*, 142, 1890–1903, <https://doi.org/10.1002/qj.2782>, <http://dx.doi.org/10.1002/qj.2782>, 2016.
- Gray, L. J., Scaife, A. A., Mitchell, D. M., Osprey, S., Ineson, S., Hardiman, S., Butchart, N., Knight, J., Sutton, R., and Kodera, K.: A lagged response to the 11 year solar cycle in observed winter Atlantic/European weather patterns, *JOURNAL OF GEOPHYSICAL RESEARCH-ATMOSPHERES*, 118, 13 405–13 420, <https://doi.org/10.1002/2013JD020062>, 2013.
- 30 Haigh, J. D. and Blackburn, M.: Solar influences on dynamical coupling between the stratosphere and troposphere, *SPACE SCIENCE REVIEWS*, 125, 331–344, <https://doi.org/10.1007/s11214-006-9067-0>, 2006.
- Hakim, G. J., Emile-Geay, J., Steig, E. J., Noone, D., Anderson, D. M., Tardif, R., Steiger, N., and Perkins, W. A.: The lastmillennium climate reanalysis project: Framework and first results, *JOURNAL OF GEOPHYSICAL RESEARCH-ATMOSPHERES*, 121, 6745–6764, <https://doi.org/10.1002/2016JD024751>, 2016.
- 35



- Hurrell, J. W., Kushnir, Y., Ottersen, G., and Visbeck, M.: An Overview of the North Atlantic Oscillation, pp. 1–35, American Geophysical Union, <https://doi.org/10.1029/134GM01>, <http://dx.doi.org/10.1029/134GM01>, 2013.
- Ineson, S., Scaife, A. A., Knight, J. R., Manners, J. C., Dunstone, N. J., Gray, L. J., and Haigh, J. D.: Solar forcing of winter climate variability in the Northern Hemisphere, *NATURE GEOSCIENCE*, 4, 753–757, <https://doi.org/10.1038/NNGEO1282>, 2011.
- 5 Jiang, H., Muscheler, R., Björck, S., Seidenkrantz, M.-S., Olsen, J., Sha, L., Sjolte, J., Eiriksson, J., Ran, L., Knudsen, K.-L., and Knudsen, M. F.: Solar forcing of Holocene summer sea-surface temperatures in the northern North Atlantic, *GEOLOGY*, 43, 203–206, <https://doi.org/10.1130/G36377.1>, 2015.
- Johnsen, S. and Vinther, B.: {ICE} {CORE} {RECORDS} | Greenland Stable Isotopes, in: Encyclopedia of Quaternary Science, edited by Elias, S. A., pp. 1250 – 1258, Elsevier, Oxford, <https://doi.org/http://dx.doi.org/10.1016/B0-44-452747-8/00345-8>,
10 <http://www.sciencedirect.com/science/article/pii/B0444527478003458>, 2007.
- Jones, P., Jonsson, T., and Wheeler, D.: Extension to the North Atlantic Oscillation using early instrumental pressure observations from Gibraltar and south-west Iceland, *INTERNATIONAL JOURNAL OF CLIMATOLOGY*, 17, 1433–1450, [https://doi.org/10.1002/\(SICI\)1097-0088\(19971115\)17:13<1433::AID-JOC203>3.0.CO;2-P](https://doi.org/10.1002/(SICI)1097-0088(19971115)17:13<1433::AID-JOC203>3.0.CO;2-P), 1997.
- Jungclauss, J. H., Lorenz, S. J., Timmreck, C., Reick, C. H., Brovkin, V., Six, K., Segschneider, J., Giorgetta, M. A., Crowley, T. J., Pongratz, J., Krivova, N. A., Vieira, L. E., Solanki, S. K., Klocke, D., Botzet, M., Esch, M., Gayler, V., Haak, H., Raddatz, T. J., Roeckner, E., Schnur, R., Widmann, H., Claussen, M., Stevens, B., and Marotzke, J.: Climate and carbon-cycle variability over the last millennium, *Climate of the Past*, 6, 723–737, <https://doi.org/10.5194/cp-6-723-2010>, <http://www.clim-past.net/6/723/2010/>, 2010.
- Jungclauss, J. H., Bard, E., Baroni, M., Braconnot, P., Cao, J., Chini, L. P., Egorova, T., Evans, M., González-Rouco, J. F., Goosse, H., Hurrell, G. C., Joos, F., Kaplan, J. O., Khodri, M., Klein Goldewijk, K., Krivova, N., LeGrande, A. N., Lorenz, S. J., Luterbacher, J., Man, W., Maycock, A. C., Meinshausen, M., Moberg, A., Muscheler, R., Nehrbass-Ahles, C., Otto-Bliesner, B. I., Phipps, S. J., Pongratz, J., Rozanov, E., Schmidt, G. A., Schmidt, H., Schmutz, W., Schurer, A., Shapiro, A. I., Sigl, M., Smerdon, J. E., Solanki, S. K., Timmreck, C., Toohey, M., Usoskin, I. G., Wagner, S., Wu, C.-J., Yeo, K. L., Zanchettin, D., Zhang, Q., and Zorita, E.: The PMIP4 contribution to CMIP6 – Part 3: The last millennium, scientific objective, and experimental design for the PMIP4 *past1000* simulations, *Geoscientific Model Development*, 10, 4005–4033, <https://doi.org/10.5194/gmd-10-4005-2017>, <https://www.geosci-model-dev.net/10/4005/2017/>, 2017.
- 20 Kodera, K. and Kuroda, Y.: A possible mechanism of solar modulation of the spatial structure of the North Atlantic Oscillation, *Journal of Geophysical Research: Atmospheres*, 110, n/a–n/a, <https://doi.org/10.1029/2004JD005258>, <http://dx.doi.org/10.1029/2004JD005258>, d02111, 2005.
- Luterbacher, J., Xoplaki, E., Dietrich, D., Jones, P. D., Davies, T. D., Portis, D., Gonzalez-Rouco, J. F., von Storch, H., Gyalistras, D., Casty, C., and Wanner, H.: Extending North Atlantic oscillation reconstructions back to 1500, *Atmospheric Science Letters*, 2, 114–124, <https://doi.org/10.1006/asle.2002.0047>, <http://dx.doi.org/10.1006/asle.2002.0047>, 2001.
- 30 Luterbacher, J., Dietrich, D., Xoplaki, E., Grosjean, M., and Wanner, H.: European seasonal and annual temperature variability, trends, and extremes since 1500, *SCIENCE*, 303, 1499–1503, <https://doi.org/10.1126/science.1093877>, 2004.
- Moffa-Sanchez, P., Born, A., Hall, I. R., Thornalley, D. J. R., and Barker, S.: Solar forcing of North Atlantic surface temperature and salinity over the past millennium, *NATURE GEOSCIENCE*, 7, 275–278, <https://doi.org/10.1038/ngeo2094>, 2014.
- 35 Moreno-Chamarro, E., Zanchettin, D., Lohmann, K., and Jungclauss, J. H.: An abrupt weakening of the subpolar gyre as trigger of Little Ice Age-type episodes, *Climate Dynamics*, 48, 727–744, <https://doi.org/10.1007/s00382-016-3106-7>, <https://doi.org/10.1007/s00382-016-3106-7>, 2017.



- Muscheler, R., Joos, F., Beer, J., Müller, S. A., Vonmoos, M., and Snowball, I.: Solar activity during the last 1000 yr inferred from radionuclide records, *Quaternary Science Reviews*, 26, 82 – 97, <https://doi.org/http://dx.doi.org/10.1016/j.quascirev.2006.07.012>, <http://www.sciencedirect.com/science/article/pii/S0277379106002460>, 2007.
- Muscheler, R., Adolphi, F., Herbst, K., and Nilsson, A.: The Revised Sunspot Record in Comparison to Cosmogenic
5 Radionuclide-Based Solar Activity Reconstructions, *Solar Physics*, 291, 3025–3043, <https://doi.org/10.1007/s11207-016-0969-z>, <http://dx.doi.org/10.1007/s11207-016-0969-z>, 2016.
- Ortega, P., Lehner, F., Swingedouw, D., Masson-Delmotte, V., Raible, C. C., Casado, M., and Yiou, P.: A model-tested North Atlantic Oscillation reconstruction for the past millennium, *NATURE*, 523, 71+, <https://doi.org/10.1038/nature14518>, 2015.
- Pinto, J. G. and Raible, C. C.: Past and recent changes in the North Atlantic oscillation, *WILEY INTERDISCIPLINARY REVIEWS-
10 CLIMATE CHANGE*, 3, 79–90, <https://doi.org/10.1002/wcc.150>, 2012.
- Scaife, A. A., Ineson, S., Knight, J. R., Gray, L., Kodera, K., and Smith, D. M.: A mechanism for lagged North Atlantic climate response to solar variability, *Geophysical Research Letters*, 40, 434–439, <https://doi.org/10.1002/grl.50099>, <http://dx.doi.org/10.1002/grl.50099>, 2013.
- Schmidt, G. A., Jungclauss, J. H., Ammann, C. M., Bard, E., Braconnot, P., Crowley, T. J., Delaygue, G., Joos, F., Krivova, N. A.,
15 Muscheler, R., Otto-Bliesner, B. L., Pongratz, J., Shindell, D. T., Solanki, S. K., Steinhilber, F., and Vieira, L. E. A.: Climate forcing reconstructions for use in PMIP simulations of the last millennium (v1.0), *Geoscientific Model Development*, 4, 33–45, <https://doi.org/10.5194/gmd-4-33-2011>, <http://www.geosci-model-dev.net/4/33/2011/>, 2011.
- Schmidt, G. A., Jungclauss, J. H., Ammann, C. M., Bard, E., Braconnot, P., Crowley, T. J., Delaygue, G., Joos, F., Krivova, N. A.,
Muscheler, R., Otto-Bliesner, B. L., Pongratz, J., Shindell, D. T., Solanki, S. K., Steinhilber, F., and Vieira, L. E. A.: Climate forc-
20 ing reconstructions for use in PMIP simulations of the Last Millennium (v1.1), *Geoscientific Model Development*, 5, 185–191, <https://doi.org/10.5194/gmd-5-185-2012>, <http://www.geosci-model-dev.net/5/185/2012/>, 2012.
- Sejrup, H. P., Lehman, S. J., Haffidason, H., Noone, D., Muscheler, R., Berstad, I. M., and Andrews, J. T.: Response of Norwegian Sea temperature to solar forcing since 1000 A.D., *Journal of Geophysical Research: Oceans*, 115, n/a–n/a, <https://doi.org/10.1029/2010JC006264>, <http://dx.doi.org/10.1029/2010JC006264>, c12034, 2010.
- 25 Shindell, D. T., Schmidt, G. A., Mann, M. E., Rind, D., and Waple, A.: Solar Forcing of Regional Climate Change During the Maunder Minimum, *Science*, 294, 2149–2152, <https://doi.org/10.1126/science.1064363>, <http://science.sciencemag.org/content/294/5549/2149>, 2001.
- Sigl, M., Winstrup, M., McConnell, J. R., Welten, K. C., Plunkett, G., Ludlow, F., Buentgen, U., Caffee, M., Chellman, N., Dahl-Jensen, D., Fischer, H., Kipfstuhl, S., Kostick, C., Maselli, O. J., Mekhaldi, F., Mulvaney, R., Muscheler, R., Pasteris, D. R., Pilcher, J. R., Salzer, M.,
30 Schuepbach, S., Steffensen, J. P., Vinther, B. M., and Woodruff, T. E.: Timing and climate forcing of volcanic eruptions for the past 2,500 years, *NATURE*, 523, 543+, <https://doi.org/10.1038/nature14565>, 2015.
- Steiger, N. J., Steig, E. J., Dee, S. G., Roe, G. H., and Hakim, G. J.: Climate reconstruction using data assimilation of water isotope ratios from ice cores, *Journal of Geophysical Research: Atmospheres*, 122, 1545–1568, <https://doi.org/10.1002/2016JD026011>, <http://dx.doi.org/10.1002/2016JD026011>, 2016JD026011, 2017.
- 35 Stuiver, M., Braziunas, T., Grootes, P., and Zielinski, G.: Is There Evidence for Solar Forcing of Climate in the GISP2 Oxygen Isotope Record?, *Quaternary Research*, 48, 259 – 266, <https://doi.org/http://dx.doi.org/10.1006/qres.1997.1931>, <http://www.sciencedirect.com/science/article/pii/S0033589497919311>, 1997.



- Swingedouw, D., Terray, L., Cassou, C., Voldoire, A., Salas-Méllia, D., and Servonnat, J.: Natural forcing of climate during the last millennium: fingerprint of solar variability, *Climate Dynamics*, 36, 1349–1364, <https://doi.org/10.1007/s00382-010-0803-5>, <https://doi.org/10.1007/s00382-010-0803-5>, 2011.
- Swingedouw, D., Mignot, J., Ortega, P., Khodri, M., Menegoz, M., Cassou, C., and Hanquiez, V.: Impact of explosive volcanic eruptions on the main climate variability modes, *GLOBAL AND PLANETARY CHANGE*, 150, 24–45, <https://doi.org/10.1016/j.gloplacha.2017.01.006>, 2017.
- Thieblemont, R., Matthes, K., Omrani, N.-E., Kodera, K., and Hansen, F.: Solar forcing synchronizes decadal North Atlantic climate variability, *NATURE COMMUNICATIONS*, 6, <https://doi.org/10.1038/ncomms9268>, 2015.
- Trouet, V., Esper, J., Graham, N. E., Baker, A., Scourse, J. D., and Frank, D. C.: Persistent Positive North Atlantic Oscillation Mode Dominated the Medieval Climate Anomaly, *SCIENCE*, 324, 78–80, <https://doi.org/10.1126/science.1166349>, 2009.
- Vinther, B., Jones, P., Briffa, K., Clausen, H., Andersen, K., Dahl-Jensen, D., and Johnsen, S.: Climatic signals in multiple highly resolved stable isotope records from Greenland, *Quaternary Science Reviews*, 29, 522 – 538, <https://doi.org/http://dx.doi.org/10.1016/j.quascirev.2009.11.002>, <http://www.sciencedirect.com/science/article/pii/S0277379109003655>, 2010.
- 15 Vinther, B. M., Johnsen, S. J., Andersen, K. K., Clausen, H. B., and Hansen, A. W.: NAO signal recorded in the stable isotopes of Greenland ice cores, *Geophysical Research Letters*, 30, n/a–n/a, <https://doi.org/10.1029/2002GL016193>, <http://dx.doi.org/10.1029/2002GL016193>, 1387, 2003.
- Vinther, B. M., Clausen, H. B., Johnsen, S. J., Rasmussen, S. O., Andersen, K. K., Buchardt, S. L., Dahl-Jensen, D., Seierstad, I. K., Siggaard-Andersen, M.-L., Steffensen, J. P., Svensson, A., Olsen, J., and Heinemeier, J.: A synchronized dating of three Greenland ice cores throughout the Holocene, *Journal of Geophysical Research: Atmospheres*, 111, n/a–n/a, <https://doi.org/10.1029/2005JD006921>, <http://dx.doi.org/10.1029/2005JD006921>, d13102, 2006.
- 20 Werner, M., Haese, B., Xu, X., Zhang, X., Butzin, M., and Lohmann, G.: Glacial–interglacial changes in H₂¹⁸O, HDO and deuterium excess – results from the fully coupled ECHAM5/MPI-OM Earth system model, *Geoscientific Model Development*, 9, 647–670, <https://doi.org/10.5194/gmd-9-647-2016>, <http://www.geosci-model-dev.net/9/647/2016/>, 2016.
- 25 White, J. W. C., Barlow, L. K., Fisher, D., Grootes, P., Jouzel, J., Johnsen, S. J., Stuiver, M., and Clausen, H.: The climate signal in the stable isotopes of snow from Summit, Greenland: Results of comparisons with modern climate observations, *Journal of Geophysical Research: Oceans*, 102, 26 425–26 439, <https://doi.org/10.1029/97JC00162>, <http://dx.doi.org/10.1029/97JC00162>, 1997.
- Woollings, T., Lockwood, M., Masato, G., Bell, C., and Gray, L.: Enhanced signature of solar variability in Eurasian winter climate, *Geophysical Research Letters*, 37, n/a–n/a, <https://doi.org/10.1029/2010GL044601>, <http://dx.doi.org/10.1029/2010GL044601>, l20805, 2010.
- 30 Zambri, B. and Robock, A.: Winter warming and summer monsoon reduction after volcanic eruptions in Coupled Model Intercomparison Project 5 (CMIP5) simulations, *Geophysical Research Letters*, 43, 10,920–10,928, <https://doi.org/10.1002/2016GL070460>, <http://dx.doi.org/10.1002/2016GL070460>, 2016GL070460, 2016.
- Zambri, B., LeGrande, A. N., Robock, A., and Slawinska, J.: Northern Hemisphere winter warming and summer monsoon reduction after volcanic eruptions over the last millennium, *Journal of Geophysical Research: Atmospheres*, 122, 7971–7989, <https://doi.org/10.1002/2017JD026728>, <http://dx.doi.org/10.1002/2017JD026728>, 2017JD026728, 2017.
- 35 Zanchettin, D., Khodri, M., Timmreck, C., Toohey, M., Schmidt, A., Gerber, E. P., Hegerl, G., Robock, A., Pausata, F. S. R., Ball, W. T., Bauer, S. E., Bekki, S., Dhomse, S. S., LeGrande, A. N., Mann, G. W., Marshall, L., Mills, M., Marchand, M., Niemeier, U., Poulain, V., Rozanov, E., Rubino, A., Stenke, A., Tsigaridis, K., and Tummon, F.: The Model Intercomparison Project on the climatic response

Clim. Past Discuss., <https://doi.org/10.5194/cp-2018-32>
Manuscript under review for journal Clim. Past
Discussion started: 3 April 2018
© Author(s) 2018. CC BY 4.0 License.



to Volcanic forcing (VolMIP): experimental design and forcing input data for CMIP6, Geoscientific Model Development, 9, 2701–2719,
<https://doi.org/10.5194/gmd-9-2701-2016>, <https://www.geosci-model-dev.net/9/2701/2016/>, 2016.



Table 1. Correlations of reconstructed NAO and PC2 of reconstructed SLP, and observed NAO, 20CR PC2 and PC3 of SLP, as well as NAO reconstructions by Ortega et al. (2015) and Luterbacher et al. (2004). All correlations are for detrended data, and p-values are calculated with the random-phase test by Ebisuzaki (1997) to take into account auto-correlation.

	Annual (DJF)	10-year low-pass	20-year low-pass
Corr(NAO_{recon} , HadCRU) 1824-1970	0.52 (p<0.01)	0.68 (p<0.01)	0.70 (p<0.01)
Corr(NAO_{recon} , NAO_{20CR}) 1851-1970	0.44 (p<0.01)	0.44 (p<0.01)	0.46 (p<0.01)
Corr($SLP_{PC2-recon}$, $SLP_{PC2-20CR}$) 1851-1970	0.24 (p<0.01)	0.53 (p<0.01)	0.58 (p<0.01)
Corr($SLP_{PC2-recon}$, $SLP_{PC3-20CR}$) 1851-1970	0.19 (p<0.01)	0.57 (p<0.01)	0.66 (p<0.01)
Corr($SLP_{PC2-recon}$, $SLP_{PC2+PC3-20CR}$) 1851-1970	0.30 (p<0.01)	0.67 (p<0.01)	0.84 (p<0.01)
Corr(NAO_{recon} , Ortega et al. MC) 1241-1969	0.49 (p<0.01)	0.43 (p<0.01)	0.37 (p<0.05)
Corr(NAO_{recon} , Ortega et al. MC) 1241-1820	0.47 (p<0.01)	0.36 (p<0.05)	0.15 (p<0.2)
Corr(NAO_{recon} , Ortega et al. CC) 1241-1969	0.36 (p<0.01)	0.35 (p<0.01)	0.40 (p<0.01)
Corr(NAO_{recon} , Ortega et al. CC) 1241-1820	0.29 (p<0.01)	0.21 (p<0.05)	0.12 (p<0.2)
Corr(NAO_{recon} , Luterbacher) 1659-1970	0.34 (p<0.01)	0.39 (p<0.01)	0.40 (p<0.01)



Table 2. Correlation between solar forcing and PC2 of SLP, with and without time lag. The first column indicate which data is used, and if any filtering is done to the data. Second column is correlation coefficients between solar forcing and PC2 of reconstructed SLP, with solar forcing either being represented by sunspot number or ^{14}C data. The third column is correlation coefficients between solar forcing and PC2 of reconstructed SLP, with solar forcing represented by sunspot number shifted for a lag of 5 years. All correlations are for detrended data, and p-values are calculated with the random-phase test by Ebisuzaki (1997) to take into account auto-correlation.

	No time lag	5-year time lag
Corr(Recon. PC2 SLP, sunspots) 1700-1970	-0.06 (p>0.1)	0.20 (p<0.01)
5-year low-pass filtered data: Corr(Recon. PC2 SLP, sunspots) 1700-1970	-0.07 (p>0.1)	0.29 (p<0.01)
20-year low-pass filtered data: Corr(Recon. PC2 SLP, sunspots) 1700-1970	0.30 (p<0.05)	0.53 (p<0.01)
20-500 year band-pass filtered data: Corr(Recon. PC2 SLP, solar activity (^{14}C)) 1241-1970	0.30 (p<0.01)	-
60-500 year band-pass filtered data: Corr(Recon. PC2 SLP, solar activity (^{14}C)) 1241-1970	0.60 (p<0.01)	-

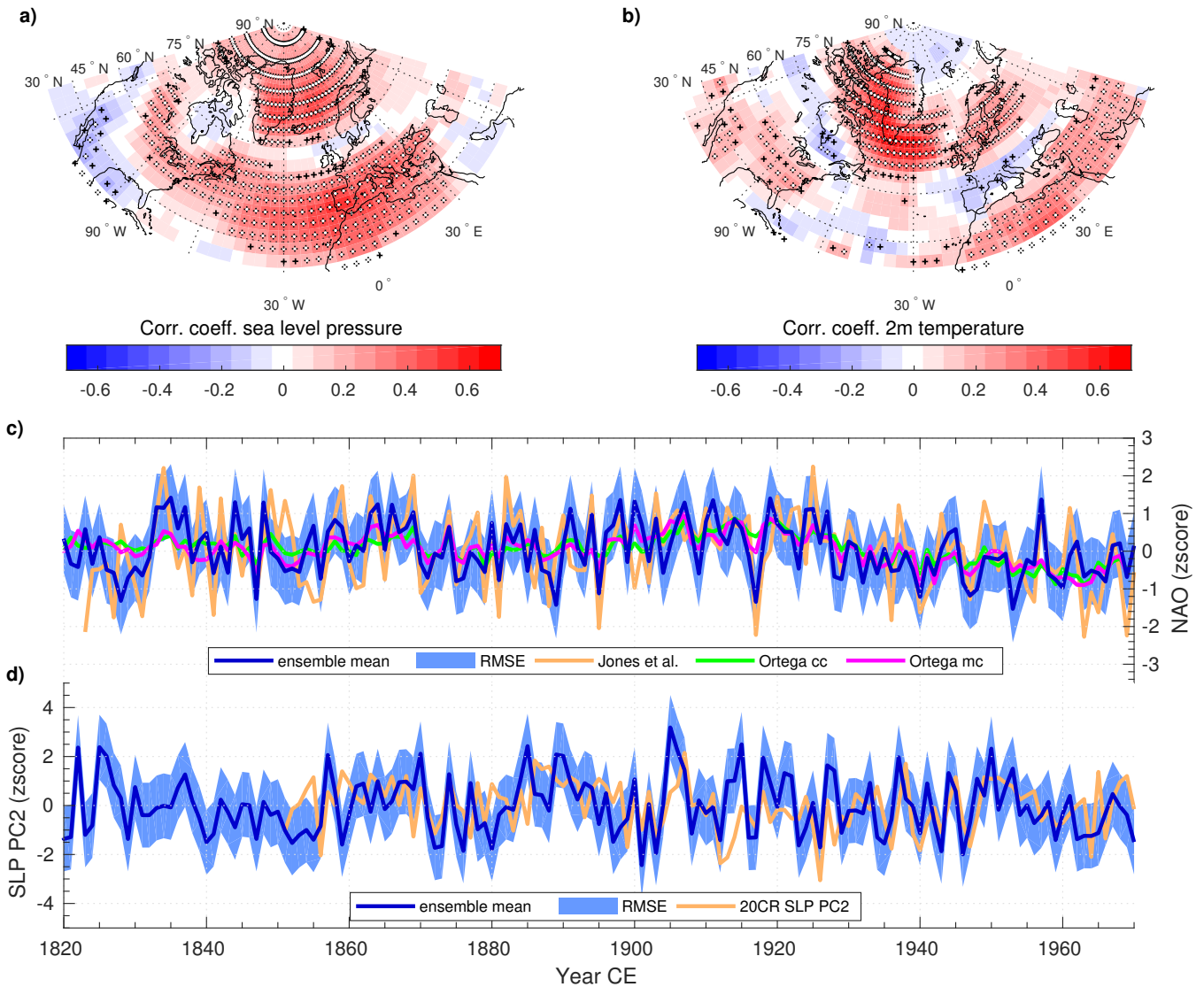


Figure 1. Evaluation of the winter circulation reconstruction. Grid point correlation between reconstructed DJF SLP (a) and T2m (b), and reanalysis data (Compo et al., 2011) (1851-1970) interpolated to the model grid (lat. x lon. $\sim 3.85^\circ \times 3.85^\circ$). The white stippling indicates significance $p < 0.05$, and black stippling indicates significance $p < 0.1$. c Ensemble mean reconstructed DJF NAO (PC1 of reconstructed DJF SLP (Hurrell et al., 2013)) with Root Mean Square Error (RMSE) compared to observed DJF NAO (Jones et al., 1997), NAOcc and NAOmc by Ortega et al. (2015). (d) Ensemble mean PC2 of reconstructed DJF SLP with RMSE compared to PC2 of reanalysis DJF SLP (Compo et al., 2011).

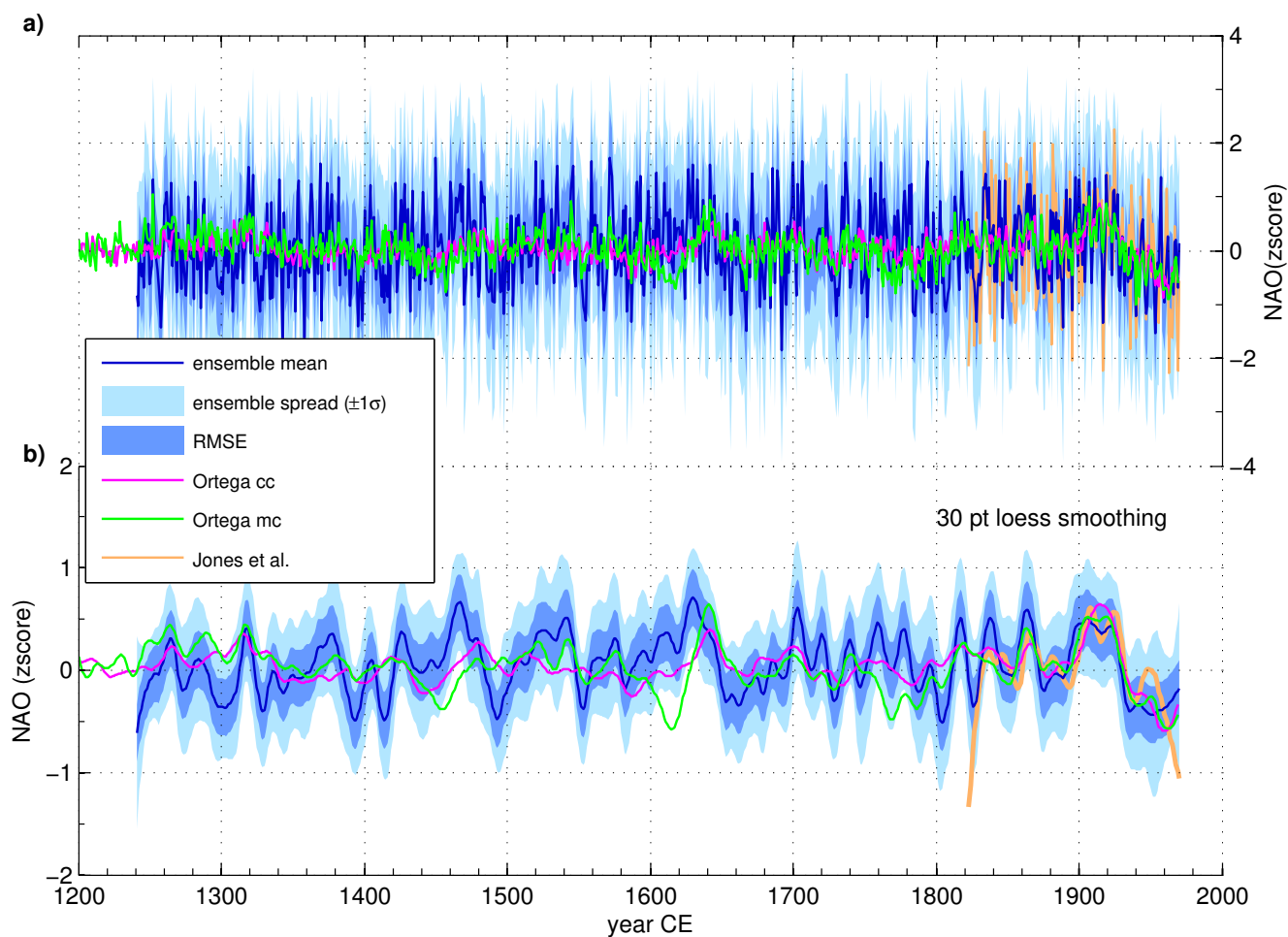


Figure 2. Comparison of instrumental and proxy-based NAO reconstructions. **a** Ensemble mean reconstructed NAO (PC1 of reconstructed SLP (Hurrell et al., 2013)) with error estimated by ensemble spread and RMSE, compared to observed NAO (Jones et al., 1997) and NAO reconstructions by Ortega et al. (2015). The amplitude of all time series are scaled to fit the decadal variability of the observed NAO. **b** Same as **a**, except filtered with a 30 point 'loess' filter.

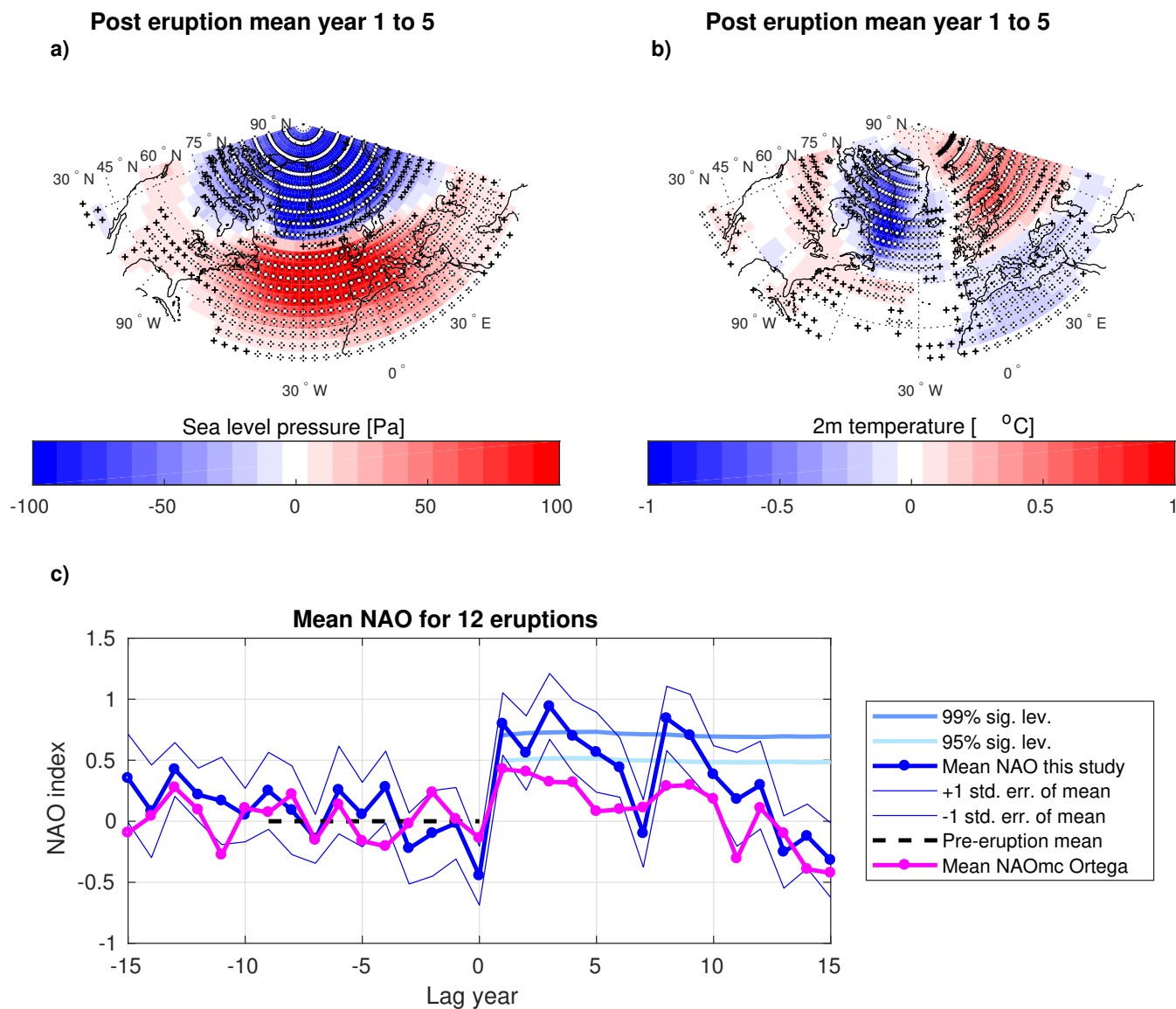


Figure 3. Superimposed epoch analysis of the mean response in atmospheric circulation to the 12 largest tropical volcanic eruptions (Sigl et al., 2015) (Table S3). The response in SLP and T2m is normalized to the mean fields of the 10 years preceding the eruption. **a** Mean DJF SLP anomalies [Pa] for the first five post eruption years. **b** Mean DJF T2m anomalies [°C] for the first five post eruption years. The white stippling indicates significant anomalies $p < 0.01$, and black stippling indicates significant anomalies $p < 0.05$ (two-tailed Student's t -test). **c** Mean response in reconstructed NAO (blue) with the time series normalized to the mean NAO of the 10 years preceding the eruption. For comparison the same analysis is carried out for the NAOmc reconstruction (magenta) by Ortega et al. (2015). The significance levels in **c** are estimated from 100,000 random samples of 12 years drawn from the reconstructed NAO. See Figure S6 for significance levels for NAOmc.

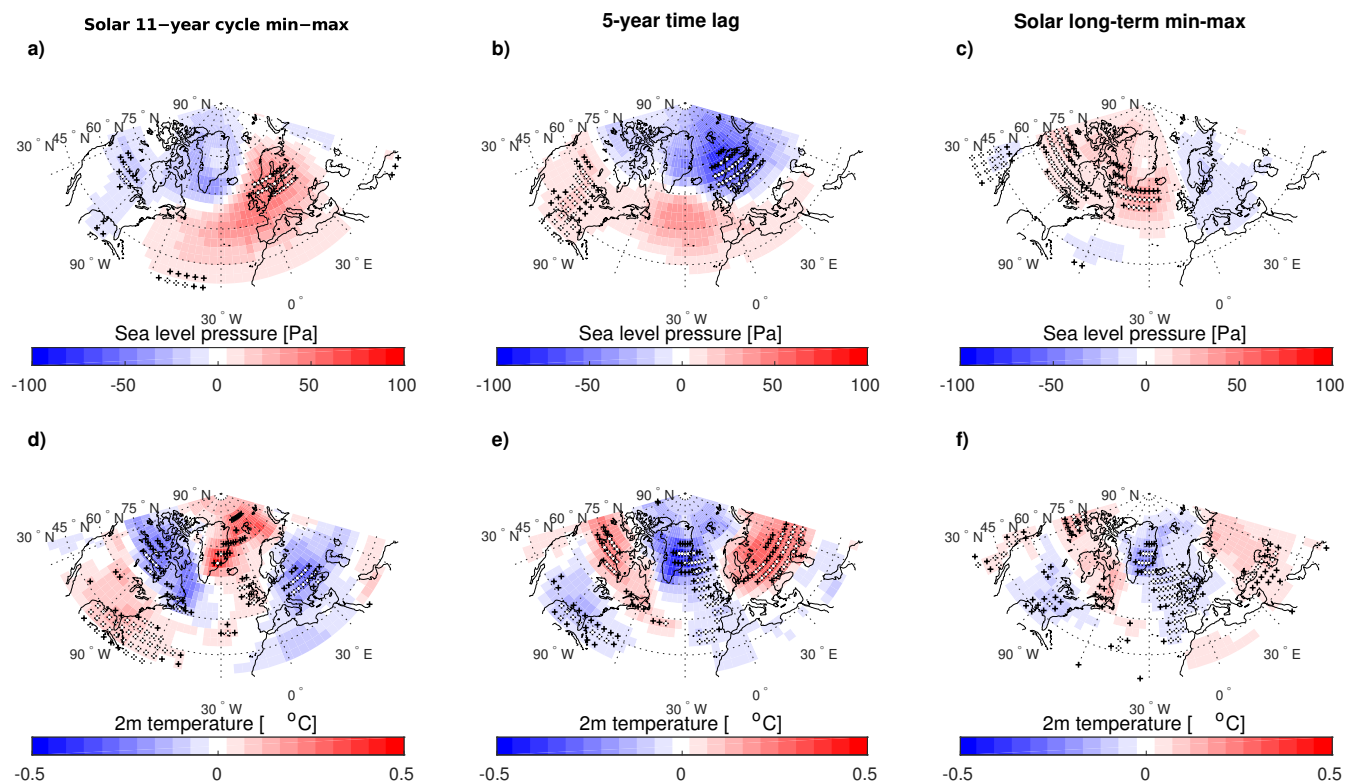


Figure 4. Reconstructed atmospheric response to solar forcing. **a** DJF SLP anomalies [Pa] in response to the 11-year solar cycle (solar min. minus solar max. defined in Figure S8). **b** DJF SLP anomalies [Pa] in response to the 5-year lagged 11-year solar cycle (solar min. minus solar max.). **c** DJF SLP anomalies [Pa] in response to the long-term solar forcing (solar min. minus solar max. defined in Figure S9). **d, e, f** corresponding figures to **a, b, c**, but for T2m [°C]. The white stippling indicates significant anomalies $p < 0.05$, and black stippling indicates significant anomalies $p < 0.1$ (two-tailed Student's t -test).

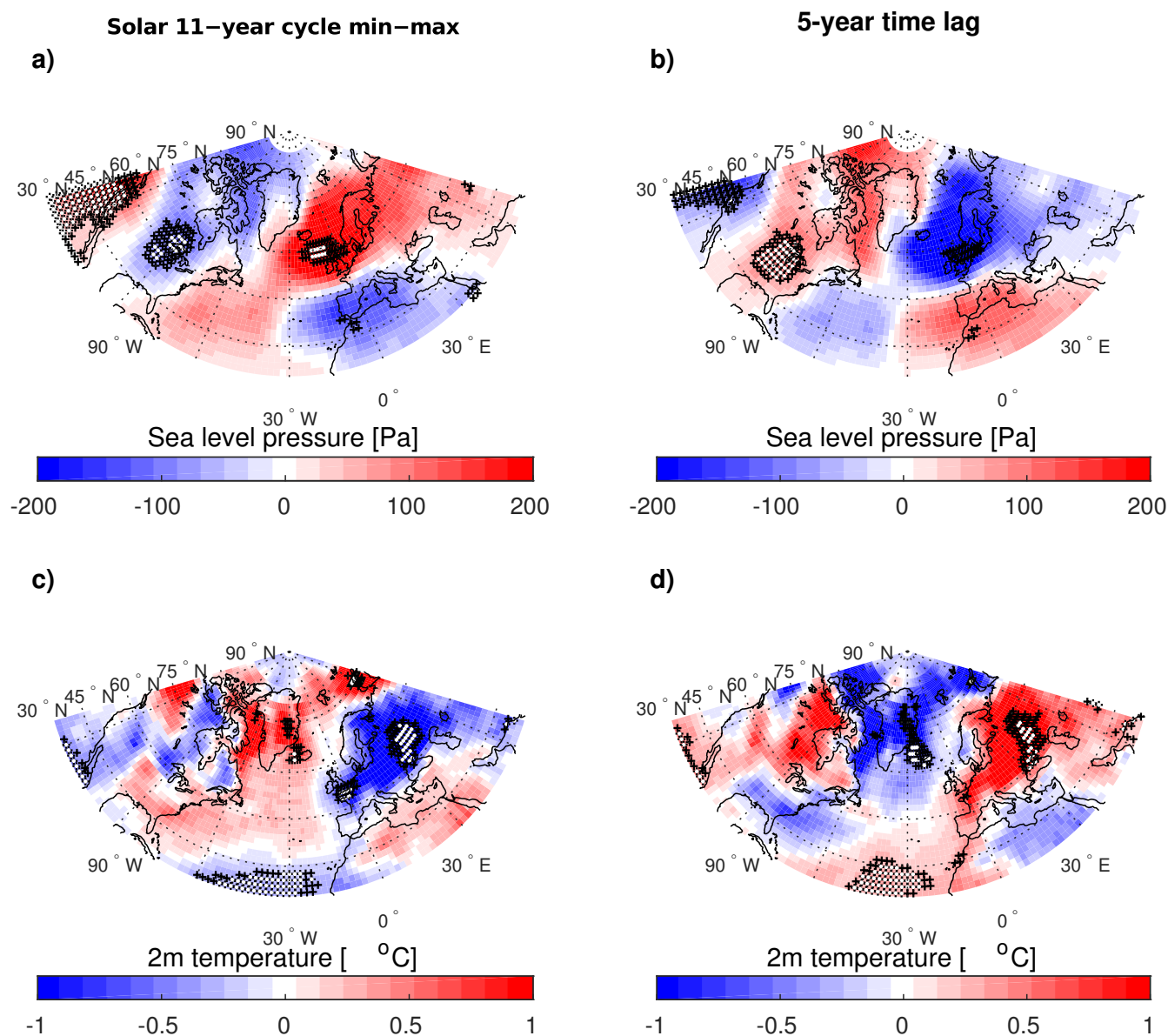


Figure 5. 20CR (1948-2010) atmospheric response to solar forcing. **a** DJF SLP anomalies [Pa] in response to the 11-year solar cycle (solar min. minus solar max. defined in Figure S10). **b** DJF SLP anomalies [Pa] in response to the 5-year lagged 11-year solar cycle (solar min. minus solar max.). **c, d** corresponding figures to **a, b**, but for T2m [°C]. The white stippling indicates significant anomalies $p < 0.05$, and black stippling indicates significant anomalies $p < 0.1$ (two-tailed Student's t -test). The time interval for this analysis is limited to 1948-2010 due to limitation of the data quality prior to this, although similar results can be achieved for the period 1851-2010.

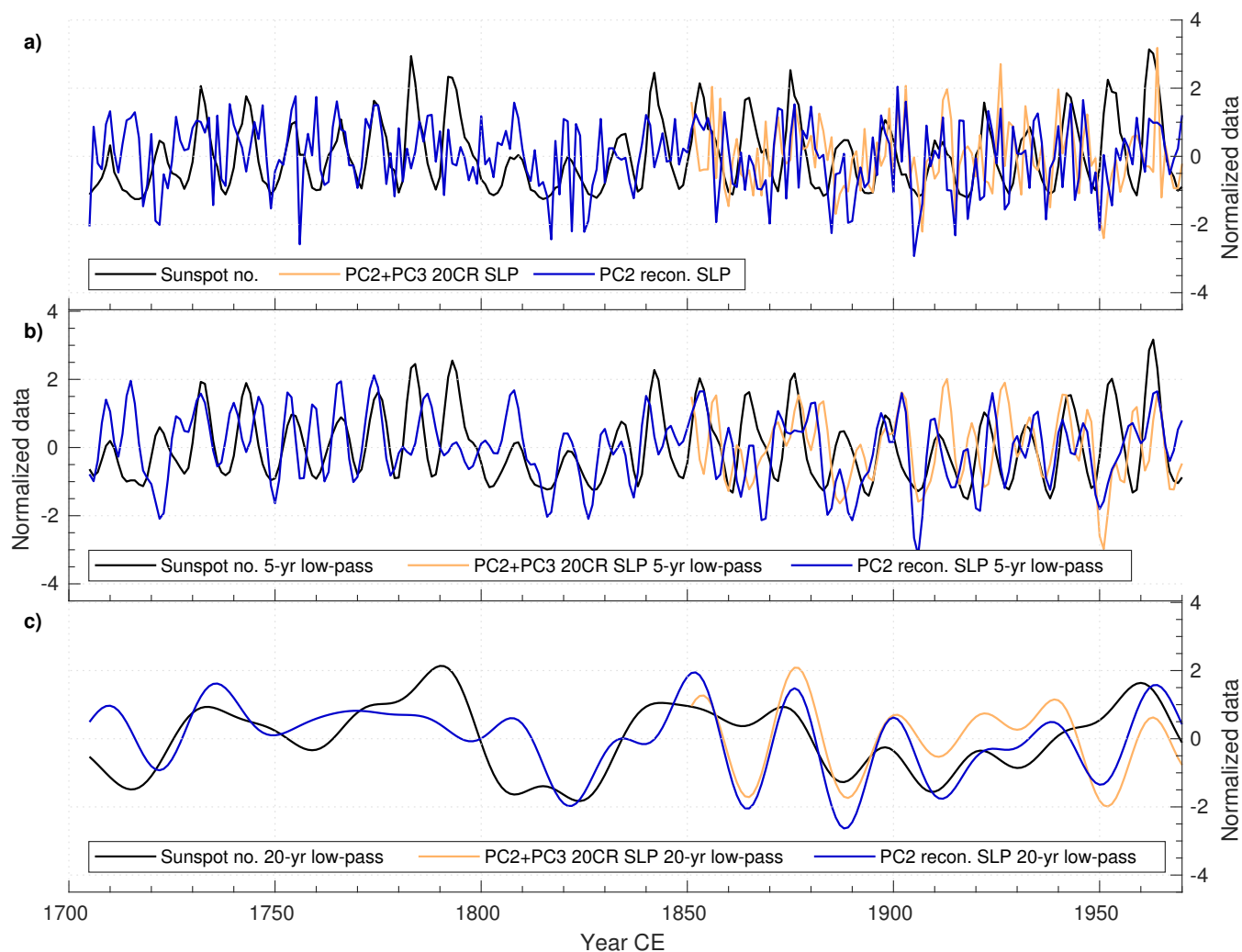


Figure 6. Reconstructed PC2 of SLP plotted with the 5-year lagged sunspot number. **a** Time series of sunspot number shifted for a 5-year time lag, PC2+PC3 of 20CR SLP (see text and Table 2) and PC2 of reconstructed SLP. **b** Same as **a**, except filtered with a 5-year low-pass filter. **c** Same as **a**, except filtered with a 20-year low-pass filter.